

Pulsed field gradient NMR study of phenol binding and exchange in dispersions of hollow polyelectrolyte capsules

Rudra Prosad Choudhury^{a)}

Institut für Physikalische Chemie, Wesfälische Wilhelms-Universität Münster, Corrensstr. 30/36, D-48149 Münster, Germany and International NRW Graduate School of Chemistry (GSC-MS), D-48149 Münster, Germany

Monika Schönhoff^{b)}

Institut für Physikalische Chemie, Wesfälische Wilhelms-Universität Münster, Corrensstr. 30/36, D-48149 Münster, Germany

(Received 31 July 2007; accepted 17 October 2007; published online 18 December 2007)

The distribution and exchange dynamics of phenol molecules in colloidal dispersions of submicron hollow polymeric capsules is investigated by pulsed field gradient NMR (PFG-NMR). The capsules are prepared by layer-by-layer assembly of polyelectrolyte multilayers on silica particles, followed by dissolution of the silica core. In capsule dispersion, ¹H PFG echo decays of phenol are single exponentials, implying fast exchange of phenol between a free site and a capsule-bound site. However, apparent diffusion coefficients extracted from the echo decays depend on the diffusion time, which is typically not the case for the fast exchange limit. We attribute this to a particular regime, where apparent diffusion coefficients are observed, which arise from the signal of free phenol only but are influenced by exchange with molecules bound to the capsule, which exhibit a very fast spin relaxation. Indeed, relaxation rates of phenol are strongly enhanced in the presence of capsules, indicating binding to the capsule wall rather than encapsulation in the interior. We present a quantitative analysis in terms of a combined diffusion-relaxation model, where exchange times can be determined from diffusion and spin relaxation experiments even in this particular regime, where the bound site acts as a relaxation sink. The result of the analysis yields exchange times between free phenol and phenol bound to the capsule wall, which are on the order of 30 ms and thus slower than the diffusion controlled limit. From bound and free fractions an adsorption isotherm of phenol to the capsule wall is extracted. The binding mechanism and the exchange mechanism are discussed. The introduction of the global analysis of diffusion as well as relaxation echo decays presented here is of large relevance for adsorption dynamics in colloidal systems or other systems, where the standard diffusion echo decay analysis is complicated by rapidly relaxing boundary conditions. © 2007 American Institute of Physics. [DOI: [10.1063/1.2807239](https://doi.org/10.1063/1.2807239)]

I. INTRODUCTION

Polyelectrolyte multilayer (PEM) capsules are novel materials with a large application potential in encapsulation and drug delivery.^{1,2} Tunable properties of the wall, which can be introduced by employing different polymeric constituents for polyion self-assembly, are one key issue for applications; another one is the fact that a large interior volume can be provided with only a small wall thickness. The permeability of the wall towards different molecular species, its dependence on size, hydrophobicity, or charge of the probe molecule, and its tunability by external parameters are important questions for further development of these capsule carriers.^{3–9}

Permeability studies performed so far can be distinguished into size determining methods on the one hand and time scale determining methods on the other hand. Concern-

ing size determination, cutoff sizes for permeation have been extracted from studies of the permeation of low molecular weight probe molecules of varying size through free standing planar membranes of PEM,^{10,11} which yielded permeation cutoffs at molecular sizes of 1–2 nm. As an alternative experimental approach, pore size distributions in polyelectrolyte multilayers were extracted from nuclear magnetic resonance cryoporometry experiments. The center of the size distribution was between 1.2 and 1.5 nm, slightly dependent on the number of layers.¹²

Concerning time scales of permeation, current approaches are time-dependent fluorescence imaging or pulsed field gradient (PFG)-NMR exchange experiments. The majority of previous permeation studies have employed probe molecules carrying fluorescent labels in laser confocal scanning microscopy (LCSM), where the time dependence of the spatial dye distribution is followed in a nonequilibrium experiment. For optical detection of the capsules, large (>micrometer) capsules are required to follow permeation in nonequilibrium experiments employing fluorescence contrast.^{5–7,9}

^{a)}Electronic mail: rudra@uni-muenster.de

^{b)}Author to whom correspondence should be addressed. Tel.: +49-2518323419. Fax: +49-2518329138. Electronic mail: schoenho@uni-muenster.de

Unlike fluorescence techniques, PFG-NMR methods do not suffer from strong restrictions concerning the probe molecules. Any molecule carrying a NMR active nucleus can be studied in a dynamic equilibrium situation of exchange, i.e., between capsule interior and exterior. Contrast between encapsulated and nonencapsulated probes is provided by the diffusion coefficient of the probe molecule, which is that of the whole capsule or that of the free solvated molecule, respectively. Analysis of echo decays obtained for different diffusion times can give information about the time scale of exchange between different sites. Based on the principle of diffusion contrast, molecular exchange between different sites has been studied in a number of different colloidal systems.^{13–16} Concerning polyelectrolyte multilayer capsules, we had previously employed PFG-NMR diffusion experiments to study large polymeric probes, i.e., dextrans, in hollow capsule dispersions.^{17,18} These polymeric probes exhibited a slow exchange between the capsule interior and exterior, and their distribution in the capsule dispersion could be analyzed. For macromolecular probe molecules with lower molecular weight, the exchange occurs on an intermediate time scale, and a quantitative analysis of exchange times and their conversion into permeation rates becomes possible. For poly(ethylene oxide), the molecular weight dependence of the exchange rate was investigated by PFG-NMR, resulting in two different mechanisms of permeation.¹⁹

Here, we study phenol as a small probe molecule with the aim to determine its distribution and exchange dynamics in capsule dispersions. Two-site models of diffusion and relaxation, respectively, are applied to analyze the exchange behavior.

From the methodological point of view, the present work gives an application example of exchange theory. In the limit of fast exchange for diffusion, typically only the fact that the molecular exchange is fast compared to the diffusion time scale (typically 10 ms) can be stated. Here, however, in the limits of fast exchange and ultrafast relaxation in one of the two sites, diffusion experiments can be evaluated and time scales extracted employing the relaxation influence on the apparent diffusion coefficient. We employ this method here to demonstrate the distribution and exchange times of fast exchanging phenol molecules in capsule dispersions.

II. MATERIALS AND METHODS

A. Materials

Poly(allylamine hydrochloride), PAH ($M_w=70\,000$ g/mol), and poly(diallyldimethyl-ammonium chloride), PDADMAC ($M_w=100\,000\text{--}150\,000$ g/mol), were purchased from Aldrich and used without further purification. Poly(sodium-4-styrenesulfonate), PSS ($M_w=70\,000$ g/mol), was purchased from ACROS. The PSS was purified by filtration (pore size of 20 μm), followed by dialysis (membrane cutoff $M_w=10\,000\text{--}20\,000$ Dalton) against pure water to remove low molecular weight fractions. Monodisperse silica particles with a radius of 200 nm were purchased from Microparticles GmbH (Berlin), deuterium oxide (99.9% isotopic purity) from Aldrich, and phenol 2,4,6-*d*₃-O-*d* from

Cambridge Isotope Laboratories. Hydrofluoric acid (HF, 40% solution) was obtained from Grüssing (Filcum, Germany). NaCl (analytical grade) was obtained from Merck. Ultrapure water purified by a three stage water purification system (Milli Q, Millipore) with a resistivity of around 18 M Ω cm was employed for all solutions. The polyelectrolytes were dissolved in 0.5M aqueous NaCl solution, where the concentration of the polyelectrolyte was 0.2 wt %.

B. Capsule preparation

Hollow capsules of PAH/PSS multilayers were prepared in two steps. In the first step assembly of multilayers on the surface of silica particle was performed by the layer-by-layer technique. Each polyelectrolyte layer was prepared by adsorption from the respective polyelectrolyte solution followed by washing of excess polyelectrolyte. Adsorption and subsequent washing cycles were carried out with the method of centrifugation-redispersion, a procedure described earlier.^{20,21} The concentration of the SiO₂ particle dispersions was kept below 2 wt % in all preparation steps to avoid coagulation during coating. As a first layer PDADMAC was adsorbed, which—in contrast to PAH—provides a stable layer on the silica surface. The adsorption of a polyelectrolyte layer was achieved by adding 5 ml of silica particle dispersion dropwise into 30 ml of the polyelectrolyte solution. After an adsorption time of 15 min under stirring, excess polyelectrolyte was removed by centrifugation and supernatant removal, and particles were redispersed in water. This washing procedure was repeated three times, before the next polyelectrolyte was adsorbed. Alternating layers of PSS and PAH were then adsorbed until a total of ten layers were deposited. Each adsorption step was confirmed by monitoring the particle size as well as the ζ -potential in a Zetasizer 3000 HSA and Zetasizer 4 (both Malvern Instruments), respectively. For removal of the silica core the coated particles were dissolved in 0.5 M hydrofluoric acid, which leads to decomposition of the silica core.¹

The remaining capsules were washed in centrifugation-decant-redispersion steps until the pH of the decanted liquid was neutral. Complete core removal was verified by energy dispersive x-ray spectroscopy (EDX) analysis and the quality of the capsules was examined by transmission electron microscopy (TEM).

To prepare samples for the NMR experiments, the water in the sample was exchanged for D₂O by six to seven washing cycles. The volume fraction of the capsules in the sample reported here was based on the initial silica particle weight fraction of the colloid dispersion, assuming negligible losses of capsules during the core dissolution process. Dispersions were prepared with 2% v/v capsules and with a phenol concentration (c_{ph}) varying from 0.2 to 1.2 wt %.

C. NMR measurements

¹H diffusion and relaxation experiments were performed on a 400 MHz Avance NMR spectrometer (Bruker) in a probe head equipped with field gradient coils (DIFF 30, Bruker) providing a maximum gradient strength of 1200 G/cm. All measurements were done at room tempera-

ture (22.5 °C). The gradient coils were cooled by a water circulation unit (Haake) that also served to control the sample temperature. Under these conditions, no influence of convection on the diffusion experiment is observed, as ensured by control experiments. The spin lattice relaxation time (T_1) was measured by inversion recovery experiments [$\pi-\tau-\pi/2$ -acquisition]. The spin-spin relaxation time (T_2) was measured by the Carr-Purcell-Meiboom-Gill (CPMG) sequence [$\pi/2-(\tau-\pi-\tau)_n$ -echo]. The pulsed field gradient method was applied to measure the self-diffusion of the phenol capsule dispersion. A stimulated echo sequence [$\pi/2-\tau-\pi/2-T-\pi/2-\tau$ -echo] was used in combination with two gradient pulses of duration δ and gradient strength g , applied during each delay τ . The spacing between the two gradient pulses is the diffusion time (Δ), which was varied between 20 and 1000 ms, while τ was constant, $\tau=5$ ms.

III. THEORY OF MOLECULAR EXCHANGE IN DIFFUSION AND RELAXATION EXPERIMENTS

A. Spin-spin relaxation and diffusion in homogeneous systems

In a diffusion experiment the measured echo intensity for a spin in a homogeneous system, where the respective molecule undergoes simple Gaussian diffusion can be described by

$$I(k) = I_0 \exp(-R_e \Delta) \exp(-Dk), \quad (1)$$

where Δ is the diffusion time, R_e is the effective relaxation rate, and D is the self-diffusion coefficient. k can be written as

$$k = \gamma^2 g^2 \delta^2 \left(\Delta - \frac{\delta}{3} \right), \quad (2)$$

where γ is the gyromagnetic ratio of the nucleus, g is the gradient strength, and δ is the gradient pulse duration. In a stimulated echo pulse sequence the effective relaxation rate R_e depends on both relaxation times T_1 and T_2 and is given by¹³

$$R_e = \frac{1}{T_e} = \frac{1}{\Delta} \left(\frac{2\tau}{T_2} + \frac{T}{T_1} \right). \quad (3)$$

In a spin-spin relaxation experiment, the echo decay can be described by

$$I(t) = I_0 \exp(-R_2 t), \quad (4)$$

with t the delay and R_2 the spin-spin relaxation rate, which is the inverse of spin-spin relaxation time T_2 . In a unified formalism of spin-spin relaxation and diffusion experiments the decay of the echo intensity can be represented as

$$I(x) = I_0 p_0 \exp(-rx), \quad (5)$$

where x is the independent variable. In case of a relaxation measurement, x is time (t) and in case of a diffusion experiment x is k given by Eq. (2). r is the decay constant, i.e., R_2 or D for relaxation or diffusion, respectively. $p_0=1$ for relaxation and $p_0=\exp(-R_e \Delta)$ for diffusion experiments, where it describes the effect of additional signal loss due to relaxation.

B. Heterogeneous systems: Two-site model

In a system, where a molecule can exist in two separate sites A and B , exchange between the sites affects the above equations. In either site the molecule is characterized by a diffusion coefficient $D_{A,B}$ and the relaxation times $T_{1A,B}$ and $T_{2A,B}$. In binding studies on colloidal particles, site A can be assigned to the probe molecules in solution with the above parameters identical to those of the probe molecule in D_2O and a mean residence time in this site τ_A . Site B then describes the bound state of the probe molecules associated to the particle, which diffuses with D_B , the diffusion coefficient of the particle. The mean residence time in the bound state is τ_B . The probability of finding the molecule in a given site i is f_i , which is given by

$$f_{A,B} = \frac{\tau_{A,B}}{\tau_A + \tau_B}. \quad (6)$$

The exchange time τ_{ex} between the sites A and B can be defined as

$$\frac{1}{\tau_{ex}} = \frac{1}{\tau_A} + \frac{1}{\tau_B}. \quad (7)$$

C. General case of intermediate exchange

In the general case, molecular exchange has to be considered, and the observed relaxation rates and diffusion coefficients are changed, while the characteristic values of $R_{eA,B}$, $R_{2A,B}$ and $D_{A,B}$ in the respective sites A and B are unaffected by this exchange. A theory of intermediate exchange in a two-site model and the effect on diffusion experiments was developed by Kärger.^{22,23} On the other hand, Woessner described the effect of intermediate exchange on spin-spin relaxation experiments.²⁴ Here, we present both these theories in a unified description of intermediate exchange in diffusion and spin-spin relaxation experiments.

In a system where a spin can exist in two separate environments with the same Larmor frequency and can migrate from one site to another, a general description of the normalized echo intensity decay is a superposition of two exponential functions,²³⁻²⁵

$$I(x) = p_A \exp(-xa_A) + p_B \exp(-xa_B). \quad (8)$$

Due to the influence of exchange, a_A and a_B are apparent decay constants, which are not identical to r in Eq. (5), and p_A and p_B are apparent populations.

D. Relaxation

For a relaxation experiment in a two-site system, the mathematical expressions that describe the apparent relaxation rates and the apparent population fractions are as follows:²⁴

$$a_A = C_1 - C_2, \quad (9a)$$

$$a_B = C_1 + C_2, \quad (9b)$$

in which

$$C_1 = \frac{1}{2} \left(\frac{1}{T_{2A}} + \frac{1}{T_{2B}} + \frac{1}{\tau_B} + \frac{1}{\tau_B} \right), \quad (10a)$$

$$C_2 = \frac{1}{2} \left[\left(\frac{1}{T_{2B}} - \frac{1}{T_{2A}} + \frac{1}{\tau_B} - \frac{1}{\tau_A} \right) + \frac{4}{\tau_A \tau_B} \right]^{1/2}, \quad (10b)$$

and

$$p_B = 1 - p_A = \frac{1}{2} - \frac{1}{4} \left[(f_A - f_B) \left(\frac{1}{T_{2A}} - \frac{1}{T_{2B}} \right) + \frac{1}{\tau_A} + \frac{1}{\tau_B} \right] \Big/ C_2. \quad (11)$$

A limiting case of intermediate exchange is found for $T_{2B} < \tau_{ex} \ll T_{2A}$: The theory of exchange in relaxation experiments in the particular case where the intrinsic relaxation times are very different and the exchange time is intermediate has been described by Woessner.²⁴ In this regime, the observed decay in a spin-spin relaxation experiment is biex-

ponential, with two apparent relaxation times $T_{appA} = 1/a_A$ and $T_{appB} = 1/a_B$ and respective population fractions given by²⁴

$$T_{appA} = \tau_A, \quad (12a)$$

$$T_{appB} = T_{2B}, \quad (12b)$$

and

$$p_A = f_A, \quad p_B = f_B, \quad (12c)$$

where f_A and f_B are the true molecular fractions in sites A and B, respectively.

E. Diffusion

In case of diffusion experiments, the effect of two-site exchange on the echo decay was described by Kärger.^{22,23} In the limit of short gradient pulses ($\delta \ll \Delta$) the echo decay follows Eq. (8), and the apparent decay constants are given by²³

$$a_{A,B} = \frac{1}{2} \left\{ (D_A + D_B) + \frac{\Delta}{k} \left(\frac{1}{T_{eA}} + \frac{1}{T_{eB}} + \frac{1}{\tau_B} + \frac{1}{\tau_A} \right) \right. \\ \left. \mp \sqrt{\left(D_B - D_A \right) + \frac{\Delta}{k} \left(\frac{1}{T_{eB}} - \frac{1}{T_{eA}} + \frac{1}{\tau_B} - \frac{1}{\tau_A} \right)} \right\}^2 + \frac{4\Delta^2}{\tau_A \tau_B k^2} \Bigg\}. \quad (13)$$

Here, T_{eA} and T_{eB} are the effective relaxation times, given by Eq. (3) for the probe molecule in sites A and B, respectively. The apparent populations are given by

$$p_B = 1 - p_A \\ = \frac{1}{(a_B - a_A)} \left\{ f_A \left(a_A + \frac{\Delta}{T_{eB} k} \right) + f_B \left(a_B + \frac{\Delta}{T_{eB} k} \right) - a_A \right\}. \quad (14)$$

According to the above description, in the intermediate exchange case, the observed properties, such as apparent relaxation rates and apparent diffusion coefficients of exchanging molecules are complex functions of different parameters, e.g., residence times, population fractions, and diffusion coefficients and relaxation rates of the nuclei in the respective sites. Two simple limiting cases can occur.

F. Fast exchange

If the exchange between the two sites is fast compared to the diffusion and relaxation time scale, then Eq. (8) becomes a single exponential decay with a mean decay constant r_m given as

$$r_m = f_A r_A + f_B r_B. \quad (15)$$

This implies that the observed parameter, i.e., relaxation rate or diffusion coefficient, is a weighted average of the respective decay constants r_A and r_B in either site.

G. Slow exchange

If the molecular exchange between the sites is slow compared to the relevant experimental time scale, the echo decays in a PFG-NMR or a T_2 relaxation experiment are superpositions of the corresponding signal decay [see Eq. (5)] of molecules in either site. This is known as slow exchange regime and the normalized echo decay can be written as

$$I(x) = p_A \exp(-r_A x) + p_B \exp(-r_B x). \quad (16)$$

In relaxation experiments the apparent fractions p_A and p_B equal the true molecular fractions f_A and f_B . In diffusion experiments the influence of relaxation has to be considered, which occurs during the delays in the pulse sequence and is described by the effective relaxation time T_e , see Eq. (3). Thus, the apparent fractions in diffusion experiments are given by

$$p_{A,B} = f_{A,B} \exp(-\Delta/T_e). \quad (17)$$

The different regimes of exchange occur depending on the relevant time scales that have to be compared to the molecular exchange time τ_{ex} . In diffusion experiments this is the diffusion time Δ , while in relaxation experiments it is the relaxation times themselves. Interesting phenomena can occur if the system is in different exchange regimes concerning different motions. The present study shows an example of this.

TABLE I. T_1 and T_2 relaxation times of phenol in capsule dispersion at different phenol concentrations.

c_{ph} (wt %)	T_1 (s)	T_2 (ms)
0.20	3.2	63.1
0.40	3.9	75.3
0.60	4.7	81.6
0.75	4.9	86.7
1.20	6.3	107.8

IV. RESULTS AND ANALYSIS

A. Phenol in water

In order to characterize the free site separately and to obtain the parameters T_{2A} , T_{1A} , and D_A , phenol dissolved in water (D_2O) is studied. It is found that for protonated phenol a coupling between different protons of the benzene ring causes severe distortions in diffusion and relaxation experiments. Therefore, selectively deuterated 2,4,6-*d*₃-phenol is employed in all experiments, where the signal of the protons in the 3,5 positions is evaluated. Phenol concentrations vary from 0.2 to 1.2 wt %. The diffusion coefficient is $D_A = (7.5 \pm 0.1) \times 10^{-10} \text{ m}^2 \text{ s}^{-1}$, independent of phenol concentration. As expected, it is not dependent on diffusion time Δ . The longitudinal relaxation time T_1 and the spin-spin relaxation time T_2 of the phenol protons in D_2O are determined to be $T_{1A} = (15.8 \pm 0.2) \text{ s}$ and $T_{2A} = (11.8 \pm 0.1) \text{ s}$. Both values are independent of phenol concentration.

B. Relaxation rates in capsule dispersion

In capsule dispersions with added phenol, relaxation experiments are performed and evaluated for the phenol protons. All spin-lattice and spin-spin relaxation measurements show single exponential behavior. The T_1 and T_2 values are given in Table I. Relaxation times of phenol in capsule dispersions are generally shorter than relaxation times of phenol in D_2O ; in addition they depend on phenol concentration. While T_1 is reduced by a factor between 2 and 5, T_2 relaxation times decrease by more than two orders of magnitude as compared to free phenol. This indicates that, in the presence of capsules, the phenol mobility is reduced, in particular, the slow isotropic motional modes determining T_2 become slow. This can be attributed to the binding of phenol to the capsules. Since all echo decays are monoexponential, the

exchange between free and bound phenol sites is fast on the relaxation time scale, and the relaxation rates can be interpreted as averages of free and bound phenol relaxation rates.

C. Diffusion experiments in capsule dispersion

Diffusion experiments are performed for different diffusion times Δ ranging from 20 to 1000 ms. All diffusion experiments show a single exponential echo decay, see Fig. 1(a). Single exponentials imply fast exchange between bound and free phenol on the time scale of Δ . However, diffusion coefficients extracted from the decays are dependent on diffusion time, which is not consistent with the fast exchange limit. We therefore define the decay constants as “apparent diffusion coefficients” D_{app} and will discuss their relevance below. Figure 1(b) gives the apparent diffusion coefficients depending on diffusion time for the sample with 0.6 wt % phenol. The values decrease with increasing Δ and seem to converge to a constant value for $\Delta > 800 \text{ ms}$.

D. Qualitative interpretation

From the above observations, it is confirmed that phenol strongly experiences the presence of the hollow capsules in the system, since capsules drastically alter the relaxation as well as the diffusion behavior as compared to phenol dissolved in D_2O . The observation of single exponential decays, both in relaxation and diffusion experiments, indicates that the exchange time τ_{ex} is very fast compared to the time scales of relaxation and diffusion. On the other hand, as D_{app} depends on Δ , the system is not completely in the limit of fast exchange. Monoexponential diffusion echo decays can result, if the exchange is fast on the diffusion time scale, i.e., $\tau_{\text{ex}} \ll \Delta$, but on the other hand relaxation leads to a reduction of the signal with increasing Δ in one of the two sites.

The short average relaxation times T_2 (see Table I) indicate a relaxation time T_{2B} , which is very short. Provided that $T_{2B} \ll \tau_{\text{ex}}$ but on the other hand $\tau_{\text{ex}} \ll \Delta$, T_{2A} , the present regime can be qualitatively explained: Due to the short T_{2B} , only the free component A is detected in the PFG experiment. With an exchange that is fast compared to Δ , however, the spatial displacement of the free molecules is influenced by exchange. Therefore the apparent diffusion coefficient is reduced as compared to D_A . The influence of the bound site becomes more prominent as Δ increases, thus causing the reduction of D_{app} . In this way the diffusion behavior, show-

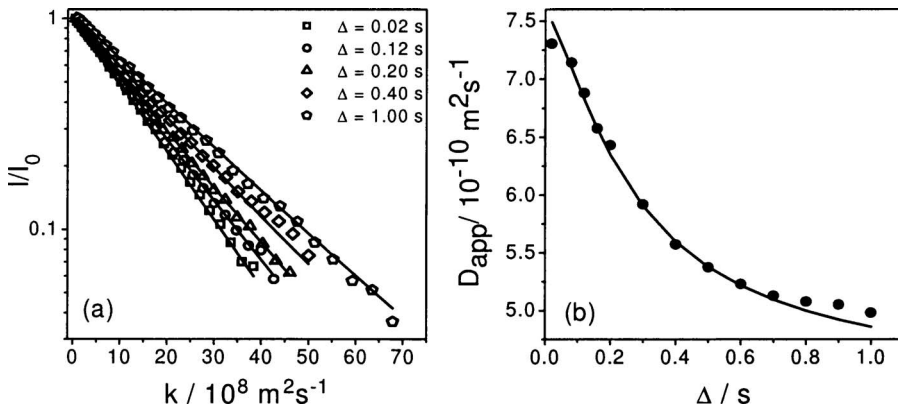


FIG. 1. (a) Symbols: Echo decays of phenol in capsule dispersion for $c_{\text{ph}} = 0.6 \text{ wt } \%$. Lines: Global fit. Note that, for clarity, only the data for a selection of Δ values are displayed. (b) Apparent diffusion coefficients. Symbols: D_{app} extracted from monoexponential fits of single echo decays. Solid line: $D_{\text{app}}(\Delta)$ calculated from the set of resulting parameters P_{res} .

ing monoexponential echo decays with apparent diffusion coefficients $D_{\text{app}}(\Delta)$ can be qualitatively explained by a regime where $T_{2B} < \tau_{\text{ex}} \ll \Delta, T_{2A}$.

E. Quantitative analysis of diffusion echo decays

For a quantitative analysis of the diffusion decay data, the model of intermediate exchange between two sites is employed. We point out that no assumptions about the time scales or regimes of exchange are made in the analysis. The diffusion coefficient and relaxation rates of the free site are taken as identical to those determined in D_2O , thus $T_{1A} = (15.6 \pm 0.2)$ s, $T_{2A} = (11.8 \pm 0.1)$ s, and $D_A = (7.5 \pm 0.1) \times 10^{-10} \text{ m}^2 \text{ s}^{-1}$. For the diffusion coefficient of the phenol in the bound site D_B , the diffusion coefficient of the capsule itself is taken. It is calculated from the Stokes-Einstein relation ($D = k_B T / 6\pi\eta R$). The radius of the capsule is assumed to be that of the silica particle before dissolution, $R = 200$ nm, as given by the manufacturer and confirmed by dynamic light scattering. Then, the calculated diffusion coefficient of the capsule is $D_B = (9.2 \pm 0.7) \times 10^{-13} \text{ m}^2 \text{ s}^{-1}$. T_{1B} is taken as a fixed input parameter as well; the value is determined by extrapolating spin-lattice relaxation rates obtained for different concentrations of phenol c_{ph} (Fig. 3) to $c_{\text{ph}} = 0$, which results in $T_{1B} = 2.8$ s. This procedure is based on the assumption that at infinitely low phenol concentration the bound site is occupied and no free phenol is present. This assumption might be questioned; however, the influence of the value of T_{1B} on the fit results is negligible. The set of fixed input parameters is thus $P_{\text{in}} = (D_A, D_B, T_{1A}, T_{2A}, T_{1B})$. By analyzing the echo decays for different Δ (Fig. 1) employing Eqs. (8), (13), and (14), the unknown parameters T_{2B} , τ_A , and τ_B are extracted. A global set of floating parameters $P_{\text{res}} = (T_{2B}, \tau_A, \tau_B)$ is optimized to fit the whole set of echo decay curves with the global set of fixed input parameters P_{in} .

The influence of errors of the input parameters P_{in} on the fit results is checked by varying the input parameters randomly within their error range. For example, as the diffusion coefficient of phenol in D_2O is determined to be $D_A = (7.5 \pm 0.1) \times 10^{-10} \text{ m}^2 \text{ s}^{-1}$, the input parameter D_A is varied from 7.4×10^{-10} to $7.6 \times 10^{-10} \text{ m}^2 \text{ s}^{-1}$. Similarly, the other input parameters are varied in their error range. The fit results turned out to be very sensitive only to the parameter D_A , the diffusion coefficient of free phenol.

The solid lines in Fig. 1(a) show an example of the result of global fitting for a selection of Δ values. The resulting parameters P_{res} are determined as the average of the results obtained with the variation of input parameters. With these values of the parameters P_{res} and P_{in} , the apparent diffusion coefficients are determined depending on diffusion time, see the solid line in Fig. 1(b). The comparison to the values extracted from monoexponential fits of single echo decays (data points) yields a good agreement.

Diffusion data obtained for other phenol concentrations are treated similarly, and the comparison of the results of the global fit procedure to the single values of D_{app} is given in Fig. 2. From the resulting parameters τ_A and τ_B , the bound fraction f_B and the exchange time τ_{ex} of phenol are calcu-

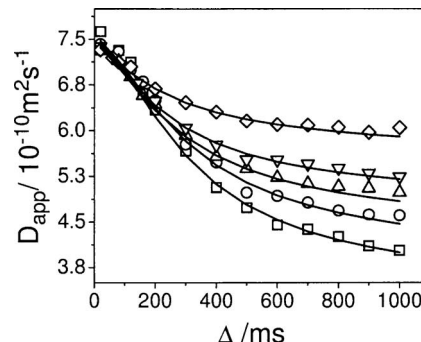


FIG. 2. Apparent diffusion coefficient of phenol at different concentrations. The symbols are values extracted from monoexponential fits of single echo decays: \square 0.2 wt %, \circ 0.4 wt %, \triangle 0.6 wt %, ∇ 0.75 wt %, and \diamond 1.2 wt % phenol. The lines are the result of the global fit of each sample with the input parameters as described in the text. Resulting parameters are given in Table II.

lated for each concentration using Eqs. (6) and (7), respectively. The results are given in Table II with their respective errors. These errors are fit errors including the effect of variation of all input parameters in their respective error range.

The values of the bound fraction are not strongly dependent on the input parameters, thus they could be determined with small errors. Less precision and a large error is obtained for the parameters T_{2B} and τ_{ex} due to strong correlations with the input parameters.

F. Interpretation of diffusion results

The bound fraction f_B is rather large, reaching almost 60% for the lowest phenol concentration. The major fraction of phenol is thus associated with the capsule. f_B shows a monotonous decrease with increasing phenol concentration. This is evidence of the onset of saturation of the capsule with phenol. The spin-spin relaxation time of the bound phenol is about $T_{2B} \approx 2$ ms without any systematic dependence on phenol concentration. It can be concluded that the dynamics of the bound fraction of phenol is strongly reduced as compared to free phenol, while it does not depend on concentration. The short T_{2B} is an indication that the phenol observed as bound fraction is not phenol freely diffusing in the interior of the capsule, since such molecules are solvated in water and should exhibit the same relaxation time T_{2B} as the free fraction. Apparently the bound fraction is dominated by phenol which is adsorbed in the capsule wall. This is consistent with the effect of saturation, since for a distribution of molecules in two chemically identical environments, i.e., the interior and the exterior of the capsules, no dependence of the fractions on concentration should appear.

TABLE II. Results obtained from global fits to the diffusion data sets of samples with different phenol concentrations.

c_{ph} (wt %)	T_{2B} (ms)	τ_{ex} (ms)	f_B
0.20	1.9 ± 0.3	23.9 ± 2.9	0.58 ± 0.01
0.40	2.1 ± 0.4	25.2 ± 4.0	0.54 ± 0.01
0.60	2.4 ± 0.4	24.3 ± 2.5	0.44 ± 0.01
0.75	2.1 ± 0.4	18.1 ± 2.8	0.38 ± 0.01
1.20	2.6 ± 0.4	31.2 ± 2.9	0.26 ± 0.01

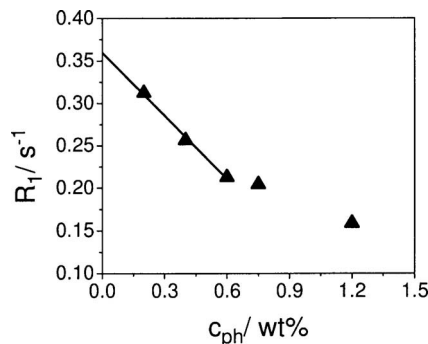


FIG. 3. Spin-lattice relaxation rate at different phenol concentrations. Triangles: experimental values; solid line: linear extrapolation of the low concentration region to $c_{ph}=0$.

The exchange time τ_{ex} is on the order of 20 ms. Here, the errors are too large to extract a systematic dependence on phenol concentration. However, the qualitative argument given above concerning the relevant time scales is well supported: The system clearly is in an intermediate exchange regime where $T_{2B} < \tau_{ex} \ll T_{2A}$, while τ_{ex} is on the order of Δ . This explains the particular observation of monoexponential echo decays in diffusion experiments, indicating fast exchange with respect to the diffusion time scale. On the other hand, the exchange is intermediate on the relaxation time scales: Due to a very short T_{2B} , the relaxation of the bound fraction is rapid, and its magnetization does not contribute to the signal in the diffusion echo decay. The apparent diffusion coefficient is thus dominated by the free phenol. With increasing Δ , however, an increasing fraction of exchanging molecules can contribute to the averaged diffusion coefficient; consequently D_{app} decreases with Δ . It appears to be essential for this regime of exchange that the magnetization of the bound fraction is not completely lost, since it is not $T_{2B} \ll \tau_{ex}$, but rather $T_{2B} < \tau_{ex}$, such that a sufficient influence of the bound fraction indirectly determines D_{app} and thus enables us to extract time scale information from the diffusion experiment, though concerning diffusion, the system is in fast exchange.

To extract more precise values for relaxation and exchange times, however, it is useful to analyze relaxation data as well, which are described in the following section.

G. T_1 relaxation

The spin-lattice relaxation of phenol in capsule dispersions is single exponential and T_1 is on the order of few seconds. T_1 shows a pronounced dependence on the phenol concentration, see Fig. 3. Since exchange times of about 10 ms are extracted from the diffusion analysis above, the exchange is fast compared to the T_1 relaxation times in either site, i.e., $\tau_{ex} \ll T_{1A}, T_{1B}$. This explains the single exponential behavior of the T_1 relaxation.

With the fractions f_A and f_B extracted from the diffusion measurements and the equation for the fast exchange average, $R_1 = f_A R_{1A} + f_B R_{1B}$, it is possible to calculate T_{1B} . The result is given in Table III. T_{1B} does not depend on c_{ph} , thus the local mobility of bound phenol is independent of the amount of phenol present in capsules. The average value is

TABLE III. T_{1B} calculated in the fast exchange limit from experimental T_1 data (Fig. 3), employing f_B obtained from global fits of diffusion decays, Table II.

c_{ph} (wt %)	T_{1B} (s)
0.20	2.1
0.40	2.3
0.60	2.5
0.75	2.2
1.20	2.3

$T_{1B}=2.2 \pm 0.2$ s. The value of T_1 which had been obtained by the extrapolation of R_1 to $c_{ph}=0$ was 2.8 s. The discrepancy is considered irrelevant for the data analysis, since T_{1B} does not have a significant influence on the fit results.

H. Analysis of T_2 relaxation data

As described above (Table I) and also in Fig. 4, T_2 experiments of phenol in capsule dispersion yield single exponential decays with apparent relaxation times of $T_{app} \sim 60-100$ ms, whereas $T_{2A}=11.8$ s for free phenol. Since T_{app} is similar to τ_{ex} , this confirms that $T_{2B} < \tau_{ex} \ll T_{2A}$.

Equations (8)–(11) were fitted by a Levenberg-Marquardt algorithm to data sets consisting of five spin-spin relaxation experiments with different phenol concentrations. The individual echo decays are described by different functions, each with corresponding population fractions taken from the diffusion data analysis. T_{2A} is a fixed input parameter with a global value of 11.8 s. The fractions f_{Ai}, f_{Bi} for each phenol concentration $c_{ph,i}$ are taken from the diffusion analysis and treated as fixed parameters, too. A global set of parameters $P_{res}=(T_{2B}, \tau_{Ai})$, where ($i=1-5$), is optimized to fit the whole set of echo decays. The optimized parameters are given in Table IV; error bars again result from a variation of the input parameters within their respective error range.

The results obtained from the T_2 relaxation data confirm the fit results obtained from the diffusion analysis: Both analyses show that (i) the exchange time lies between the T_2 relaxation times of bound and free phenol and (ii) the relaxation of bound phenol (T_{2B}) is very fast. In addition, the mean residence times τ_{Ai} of phenol in the free site (Table IV) are in very good agreement with the apparent relaxation times T_{2i} (Table I). Thus, Eq. (12a) is fulfilled and the system

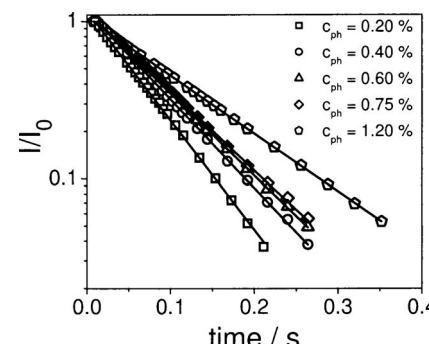


FIG. 4. Phenol ^1H echo decay curves from a CPMG experiment for different c_{ph} . The lines are the result of the global fit on all samples. Resulting parameters are given in Table IV.

TABLE IV. Results obtained from the global fits of spin-spin relaxation data for samples with different phenol concentrations. Last column: τ_B calculated under the assumption of diffusion controlled exchange, see text for details.

c_{ph} (wt %)	T_{2B} (ms)	τ_A (ms)	τ_B (ms)	τ_{ex} (ms)	$\tau_B (=1/k_-)$ (ms)
0.20		61.5 ± 0.3	85.0 ± 0.2	35.7 ± 0.2	1.2
0.40		75.9 ± 0.2	89.3 ± 0.2	38.7 ± 0.2	1.0
0.60	1.6 ± 0.3	81.8 ± 0.3	64.3 ± 0.2	36.0 ± 0.2	0.7
0.75		84.1 ± 0.2	51.5 ± 0.2	31.9 ± 0.2	0.5
1.20		111.4 ± 0.2	40.1 ± 0.2	29.7 ± 0.2	0.3

is in the limit of $T_{2B} < \tau_{ex} \ll T_{2A}$, such that in principle τ_A can be extracted directly from the single echo decays employing Eq. (12a). The limiting case described by Woessner²⁴ holds, though the fast relaxing component could not be detected in the present system. The absence of this component may be due to the fact that it decays too rapidly to be detected in the CPMG experiment.

V. DISCUSSION

With the analysis of both diffusion and the relaxation data sets, it is thus possible to quantify the distribution as well as the equilibrium exchange dynamics of phenol in capsule dispersions. Although the bound component is not directly observed in the diffusion experiment due to its very fast relaxation, the exchange causes an indirect influence of this site on the diffusion coefficient of the free component. This influence allows the determination of population distributions of phenol between the two sites, the different relaxation times, and the exchange time of the system. The fast T_2 relaxation of the bound phenol suggests that bound phenol is absorbed in the capsule wall and not enclosed in the aqueous phase in the capsule interior.

A. Third component

It is likely that a third component C of phenol is present in the aqueous interior of the capsules. This fraction should exhibit a diffusion coefficient $D_C = D_B$, since the capsule size is chosen small enough such that the spatial displacement of the total capsule within Δ is large compared to the capsule radius. A relative fraction $f_C/(f_A + f_C)$ of this component can be assumed to be similar to the volume fraction occupied by capsules, since the chemical potential and thus the concentration of phenol should be identical in sites A and C . Then, it follows that only a few percent of phenol is present in site C . This fraction is too small to be separated from the two major fractions A and B , which either have the same relaxation rate or the same diffusion coefficient, respectively.

B. Distribution of phenol

From the bound fraction f_B the total amount of bound phenol can be calculated. In Fig. 5, this adsorbed amount is given depending on the total phenol concentration. At low c_{ph} a linear increase of the adsorbed amount with c_{ph} is observed. At higher total phenol concentrations the onset of saturation of the wall with phenol is apparent, since the adsorbed amount converges towards a plateau.

The linear behavior at low concentration is easily explained by a partition coefficient of phenol between the aqueous phase and the capsule wall, which is independent of concentration. Considering the capsule wall as a hydrophobic material, this partitioning can be compared to the octanol-water partition coefficient P_{OW} , which is commonly employed to describe the hydrophilic/hydrophobic nature of small solute molecules. For phenol $\log(P_{OW}) = 1.46$.²⁶

With this value, the concentration of phenol in a hydrophobic (octanol) environment in equilibrium with water would be 30 times higher than the concentration in the water phase. Assuming a wall thickness of 10 nm and calculating the ratio of the concentrations in the wall and the aqueous phase for the initial linear region of the adsorption isotherm yields a partition coefficient P_{CW} between capsule wall material and water of 190, corresponding to $\log(P_{CW}) = 2.3$. The conclusion is that a particularly large fraction of phenol incorporates into the wall, much more than expected for a hydrophobic phase in equilibrium with water. Possibly hydrophobic interaction is not the dominant binding mechanism, and the OH group might have a specific interaction with the sulfonate groups.

At high total phenol concentrations saturation of the wall is seen, and the phenol concentration in the capsule wall is about one molecule per 150 \AA^3 . For pyrene in polyelectrolyte multilayers, Tedeschi *et al.* observed a density of 1 molecule per 7000 \AA^3 .²⁷ The much larger density of phenol in multilayers can be attributed to the OH group in the molecule, which might lead to direct interaction with free sulfate groups. Thus, the binding mechanism of phenol into the multilayers does not only involve hydrophobic interactions. This fact is therefore clearly evident from both concentration regions discussed here.

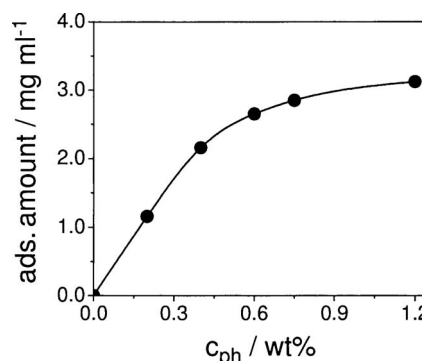


FIG. 5. Adsorbed amount of bound phenol in 1 ml capsule dispersion depending on total phenol concentration. The solid line is a guide to the eye.

The precise concentration of capsules in the dispersion is hard to determine, since losses of particles or capsules during the preparation steps slightly reduce the initial amount. The concentration given here is an upper limit of capsule concentration and is $c_{\text{caps}}=2$ vol %. However, any corrections due to a lower capsule concentration would imply even higher phenol concentrations in the wall material.

C. Exchange mechanism

The exchange time scale extracted from the relaxation experiments can give information about the mechanism of exchange between free phenol and phenol bound in the capsule wall. A simple comparison can be made by assuming an exchange process controlled by the diffusive transport of free phenol to the capsule surface. Under the assumption of immediate incorporation of a phenol molecule encountering a capsule surface by diffusion, a diffusion-controlled time scale can be calculated.¹³ For example, for the lowest concentration, this results in $\tau_B=1.2$ ms. Data for other concentrations are given in Table IV. This calculated residence time is an order of magnitude faster than that found experimentally. It is thus much more likely that the exchange is controlled by the mobility of the bound phenol in the wall rather than by transport of free phenol to the wall.

VI. CONCLUSIONS

The diffusion-exchange behavior of phenol in monodisperse hollow polymer capsule dispersion is found to be in a particular regime of intermediate exchange, which was interpreted as intermediate exchange in a two-site system with a very fast relaxation rate in the bound site, i.e., $T_{2B} < \tau_{\text{ex}} \ll T_{2A}$, while τ_{ex} is on the order of Δ . Thus, the system is in intermediate exchange concerning both relaxation and diffusion, but due to the very fast relaxation time T_{2B} only the free site contributes to the signal, while the influence of exchange with the bound site is indirectly evident by a Δ -dependent diffusion coefficient.

This particular regime of intermediate exchange was quantitatively analyzed by a two-site model taking into account the effect of relaxation in diffusion experiments. The model explains the echo decays well and, in combination with spin-spin relaxation experiments, yields relative fractions and residence times of the probe molecules in either site. We could show that single exponential decays deliver sufficient information about the dynamics, provided that they are combined with spin-spin relaxation experiments. Thus, a quantification of the exchange dynamics becomes feasible. This type of analysis is of relevance for adsorption dynamics in colloidal systems or other systems where the standard diffusion echo decay analysis is complicated by very fast relaxation in one site.

For phenol in polyelectrolyte capsule dispersion, the results of the diffusion-relaxation analysis imply that a large fraction of phenol binds to the capsule wall. Specific inter-

action of the OH group is a potential contribution to enhanced phenol incorporation. In addition, it can be assumed that there is phenol present in the capsule interior as well; however, due to the small volume fraction of capsule interior, this fraction is not apparent in the echo decay curves. The time scale of phenol exchange between the capsule wall and free phenol is much slower than the diffusion controlled rate for free phenol incorporation. It is thus most likely controlled by the mobility of phenol in the wall.

ACKNOWLEDGMENTS

We thank Dr. D. Baither, Institute of Material Physics, WWU Münster for help with TEM characterization to ensure the capsule quality. We further thank Olle Söderman, Lund for fruitful discussions. R.P.C. is greatful to the “International Graduate School of Chemistry at the University of Münster” for a doctoral fellowship.

- ¹E. Donath, G. B. Sukhorukov, F. Caruso, S. A. Davis, and H. Möhwald, *Angew. Chem., Int. Ed.* **37**, 2202 (1998).
- ²G. B. Sukhorukov, E. Donath, S. Moya, A. S. Susha, A. Voigt, J. Hartmann, and H. Möhwald, *J. Microencapsul.* **17**, 177 (2000).
- ³A. A. Antipov, G. B. Sukhorukov, E. Donath, and H. Möhwald, *J. Phys. Chem. B* **105**, 2281 (2001).
- ⁴J. H. Dai, A. W. Jensen, D. K. Mohanty, J. Erndt, and M. L. Bruening, *Langmuir* **17**, 931 (2001).
- ⁵Y. Lvov, A. A. Antipov, A. Mamedov, H. Möhwald, and G. B. Sukhorukov, *Nano Lett.* **1**, 125 (2001).
- ⁶O. P. Tiourina, A. A. Antipov, G. B. Sukhorukov, N. L. Larionova, Y. Lvov, and H. Möhwald, *Macromol. Biosci.* **1**, 209 (2001).
- ⁷G. B. Sukhorukov, A. A. Antipov, A. Voigt, E. Donath, and H. Möhwald, *Macromol. Rapid Commun.* **22**, 44 (2001).
- ⁸C. Dejugnat and G. B. Sukhorukov, *Langmuir* **20**, 7265 (2004).
- ⁹C. Dejugnat, D. Halozan, and G. B. Sukhorukov, *Macromol. Rapid Commun.* **26**, 961 (2005).
- ¹⁰X. Y. Liu and M. L. Bruening, *Chem. Mater.* **16**, 351 (2004).
- ¹¹W. Q. Jin, A. Toutianoush, and B. Tieke, *Appl. Surf. Sci.* **246**, 444 (2005).
- ¹²F. Vacca Chávez and M. Schönhoff, *J. Chem. Phys.* **126**, 104705 (2007).
- ¹³M. Schönhoff and O. Söderman, *J. Phys. Chem. B* **101**, 8237 (1997).
- ¹⁴M. Wohlgemuth and C. Mayer, *J. Colloid Interface Sci.* **260**, 324 (2003).
- ¹⁵C. Boissier, J. E. Lofroth, and M. Nyden, *J. Phys. Chem. B* **107**, 7064 (2003).
- ¹⁶A. Bauer, S. Hauschild, M. Stolzenburg, S. Förster, and C. Mayer, *Chem. Phys. Lett.* **419**, 430 (2006).
- ¹⁷T. Adalsteinsson, W. F. Dong, and M. Schönhoff, *J. Phys. Chem. B* **108**, 20056 (2004).
- ¹⁸Y. Qiao, P. Galvosas, T. Adalsteinsson, M. Schönhoff, and P. T. Callaghan, *J. Chem. Phys.* **122**, 214912 (2005).
- ¹⁹R. P. Choudhury, P. Galvosas, and M. Schönhoff, “Molecular weight dependence of PEO permeation through the walls of hollow PE capsules” (to be submitted).
- ²⁰G. B. Sukhorukov, E. Donath, H. Lichtenfeld, E. Knippel, M. Knippel, A. Budde, and H. Möhwald, *Colloids Surf., A* **137**, 253 (1998).
- ²¹B. Schwarz and M. Schönhoff, *Colloids Surf., A* **198**, 293 (2002).
- ²²J. Kärger, *Ann. Phys.* **24**, 1 (1969).
- ²³J. Kärger, *Ann. Phys.* **27**, 107 (1971).
- ²⁴D. E. Woessner, *Concepts Magn. Reson.* **8**, 397 (1996).
- ²⁵J. Kärger, *Adv. Colloid Interface Sci.* **23**, 129 (1985).
- ²⁶H. Saito, J. Koyasu, K. Yoshida, T. Shigeoka, and S. Koike, *Chemosphere* **26**, 1015 (1993).
- ²⁷C. Tedeschi, H. Möhwald, and S. Kirstein, *J. Am. Chem. Soc.* **123**, 954 (2001).